Chinese Journal of Integrative Medicine
Available online at link.springer.com/journal/11655
Journal homepage: www.cjim.cn/zxyjhen/zxyjhen/ch/index.aspx
E-mail: cjim_en@cjim.cn

Acupuncture Research

Electroacupuncture Promotes Angiogenesis in Mice with Cerebral Ischemia by Inhibiting miR-7*

YU Qian[1], SHU Shi[2], JU Xin-yao[1], PENG Wei[3], REN Xue-qi[2], SI Shu-han[1], SONG Shi-zhen[1], XIE Xue-yun[1], FANG Bang-jiang[3], and ZHOU Shuang[1]

ABSTRACT **Objective**: To observe the angiogenesis effect of electroacupuncture (EA) at Shuigou acupoint (GV 26) in the treatment of cerebral ischemia, and explore the value of miRNA-7 (miR-7) in it. **Methods**: First, 48 mice were randomly divided into sham operation, middle cerebral artery occlusion (MCAO) model, and EA treatment groups. Then 9 mice were divided into carrier control group, miR-7 knockout group and miR-7 overexpression group (*n*=3 each group). Finally, 20 mice were divided into model and carrier control group, model and miR-7 knockout group, EA treatment and carrier control group and EA treatment and miR-7 overexpression group, with 3–6 mice in each group. The MCAO model was established in the MCAO and EA groups. Neurological deficit score and 2,3,5-triphenyltetrazolium chloride (TTC) staining were used to evaluate the severity of cerebral ischemia. Hematoxylin-eosin staining was used to describe basic pathological changes. Immunohistochemistry was used to quantify cerebral microvessel density. Real-time PCR and Western blot were used to detect the expression of miR-7 and its downstream target genes Krüppel-like factor 4/vascular endothelial growth factor (KLF4/VEGF) and angiopoietin-2 (ANG-2) in the ischemic cerebral cortex. **Results**: After EA, neurological deficit scores and infarction volumes decreased, and the density of cerebral microvessels increased. In the MCAO group, miR-7 expression was higher than that in the sham group ($P<0.01$). After EA at GV 26, miR-7 expression decreased ($P<0.01$) and the expression of downstream target genes KLF4/VEGF and ANG-2 increased as compared with the MCAO group ($P<0.01$). After EA combined with overexpression of miR-7, the expression of downstream target genes KLF4/VEGF and ANG-2 decreased compared to the control EA group ($P<0.01$). After miR-7 knockdown, the expression of KLF4/VEGF and ANG-2 increased ($P<0.05$ or $P<0.01$). **Conclusions**: EA could promote angiogenesis in MCAO mice likely by inhibiting the expression of miR-7 and relieving inhibition of downstream target genes KLF4/VEGF and ANG-2.

KEYWORDS electroacupuncture, cerebral ischemia, miRNA-7, angiogenesis, Shuigou (GV 26), acupuncture points

Cerebrovascular disease is a cerebral dysfunction caused by focal cerebral ischemia and hypoxia. It is necessary to restore the blood supply to ischemic areas to save dying neurons as soon as possible after cerebral ischemia. Using various measures to promote angiogenesis after cerebral ischemia has become a focus of research. microRNA-7 (miR-7) shows a pathological link to angiogenesis, exerting biological effects by inhibiting target genes such as Krüppel-like factor 4 (KLF4)[(1)] and angiopoietin-2 (ANG-2).[(2)] Vascular endothelial growth factor (VEGF) is also regulated by KLF4,[(1)] which can be used as a regulatory target of treatment. Acupuncture can regulate cerebral vascular relaxation and contraction, in turn regulating cerebral blood flow, alleviating cerebral edema and vasospasms and promoting angiogenesis and accelerating revascularization. It activates related brain regions and regulates cerebral blood flow in patients after stroke.[(3)] It is an important external treatment method for preventing and treating ischemic diseases. Acupuncture can promote the release of vascular inducible factors, activate signal transduction pathways related to mitosis

*Supported by the National Natural Science Foundation of China (No. 81874505)
1. School of Acupuncture-Moxibustion and Tuina, Shanghai University of Traditional Chinese Medicine, Shanghai (201203), China; 2. College of Basic Medicine, Shanghai University of Traditional Chinese Medicine, Shanghai (201203), China; 3. Department of Emergency, Longhua Hospital, Shanghai University of Traditional Chinese Medicine, Shanghai (200032), China
Correspondence to: Prof. ZHOU Shuang, E-mail: zhoushuang8008@163.com
DOI: https://doi.org/10.1007/s11655-023-3715-z

Chin J Integr Med 2024 Jun;30(6):543-550

and differentiation, and improve the proliferation and migration of vascular endothelial cells and pericytes, thus inducing angiogenesis. miR-7 may be modulated by acupuncture through promoting angiogenesis in mouse models of cerebral ischemia. Acupuncture may relieve the inhibitory effects of miR-7 on the target genes KLF4/VEGF and ANG-2 via the downregulation of miR-7 to achieve this therapeutic angiogenesis. This study aimed to explore the value of miR-7 in the evaluation of electroacupuncture (EA) at Shuigou acupoint (GV 26) in the treatment of cerebral ischemia as well as its effects on angiogenesis in a mouse model of middle cerebral artery occlusion (MCAO).

METHODS

Instruments and Reagents

The following instruments and reagents were used: brain stereotaxic instrument (Shanghai Yuyan Instruments, China); micro injector (5 μL; Sigma Aldrich, USA); tying sutures (Beijing Cinontech, China); acupuncture needles (0.18 mm × 13 mm, single use; Suzhou Huatuo Medical Instruments, China); phosphate-buffered saline (PBS), citric acid antigen repair solution, hematoxylin liquid, neutral gum, horseradish peroxidase-goat anti rabbit antibody (Wuhan Servicebio Technology Co., Ltd., China); absolute alcohol, xylene, hydrogen peroxide, chloroform, isopropanol, 75% alcohol, tris-hydroxymethyl aminomethane, glycine, methanol (Sinopharm Chemical Reagent Co., Ltd., China); bovine serum albumin, sodium dodecylsulfate-polyacrylamide gel electrophoresis (SOS-PAGE) gel preparation kit (Yeasen Biotechnology [Shanghai] Co., Ltd., China); CD34 polyclonal antibody (ImmunoWay Biotechnology Company, USA); diaminobenzidine reagent kit (Agilent Technologies, USA); TRIzol reagent (Ambion Inc., USA); microRNA reverse transcription kit, 2 × qPCR Mix for microRNA (EZBioscience, USA); SDS (Sangon Biotech); pre-stained protein ladder (10–180 kD), multicolor low range protein ladder (1.7–40 kD; Thermo Fisher Scientific, USA); phenylmethylsulphonyl fluoride (Beyotime Biotechnology, China); anti-VEGF antibody, anti-KLF4 antibody, anti-ANG2 antibody (Abcam, UK); miR-7 overexpression adeno-associated virus (AAV), miR-7 knock down AAV, overexpression control AAV, carrier control AAV (Hanbio Biotechnology Co., Ltd., China).

Animals

A total of 77 male C57BL/6J mice, specific-pathogen free (SPF) grade, 20–25 g were purchased from Beijing Vitalstar Biotechnology Co., Ltd. (certificate No. SCXK-2021-0006). Animals were housed in the animal facility of the Shanghai University of Traditional Chinese Medicine on a 12 h/12 h light/dark cycle with humidity of 30%–70%, temperature of 20–24 ℃ and free access to standard food and water for 1 week before the experiments. All experiments were approved by the Animal Ethics Committee of Shanghai University of Traditional Chinese Medicine (PZSHUTCM200807030), and monitored by the Animal Experiment Center of Shanghai University of Traditional Chinese Medicine. All procedures followed the 3R principles of animal use.[4]

MCAO Model Preparation

The preparation of the mouse MCAO model followed Hata's method.[5] Mice anesthetized with 1% pentobarbital (0.1 mg/kg) were laid supine on a heating pad. A central neck incision was performed, and the subcutaneous tissue was separated. The right carotid sheath was exposed, and the carotid artery and vagus nerve were separated. Attention was paid to avoid traction injuries to the vagus nerve. The common carotid artery (CCA) was dissociated to the bifurcation, the external carotid artery (ECA) and CCA were ligated, and the internal carotid artery (ICA) was clipped. Blood vessels were cut from the proximal end of the CCA using ophthalmic scissors. Tying sutures were inserted into the ICA about 10 mm along the CCA and stopped when slight resistance was felt to block the ipsilateral middle cerebral artery. The sutures were fixed above the CCA incision. The muscle and skin of the mice were sutured by layer after complete hemostasis, and mice were kept warm until they woke up. During the operation, the rectal temperature of the mice was maintained at 37.0 ± 0.5 ℃. A sham operation group received only separation of the blood vessels, without insertion of the tying suture. Only mice with neurological deficit score of 2–3 were included in follow-up experiments.

Animal Grouping and Handling

According to random number table method, 48 mice were randomly divided into 3 groups: a sham operation group (sham), a model group (MCAO), and an EA treatment group (EA), with 16 mice each group. Then 9 mice were divided into carrier control (NC), miR-7 knockdown (KD) and miR-7 overexpression (OE) groups (n=3 each group). Finally, 20 mice were divided into MCAO+NC , MCAO+KD, EA+NC and

EA+OE groups, with 3–6 mice in each group. In the sham group, mice were only isolated blood without ischemic treatment. MCAO modeling were inducted in the MCAO, EA, MCAO+NC, MCAO+KD, EA+NC, and EA+OE groups. In the EA, EA+NC, and EA+OE groups, MCAO model mice received acupuncture treatment at GV 26 according to the "Acupoint Map of Experimental Animals" formulated by Hua, et al.[6] The mice in each group were tested 3 days after model induction (or sham operation).

Mice in each group were caught and fixed in the same way at the same time every day to exclude the influence of factors such as grasping, fixed stimulation, and circadian rhythms on the research results and to ensure the reliability of the results.

Intervention Measures

A G6805-Ⅱ EA apparatus was connected to the GV 26 and the mice skin of the right ear root. The waveform was a dense-sparse wave with a frequency of 4/20 Hz. The stimulation intensity was set to 1 mA to maintain a slight shake in the acupuncture area. Mice were treated once immediately after model induction, then once a day for 30 min. Tissue samples were collected after 3 days of treatment.

Neurological Deficit Grading

Comprehensive grading of neurological deficits was performed according to Hun's Neurological Deficit grading, as follows:[7] 0 points, no obvious deficits; 1 point, after lifting the tail, the ischemic contralateral body bent or the ischemic contralateral forelimb could not be straightened; 2 points, mice could walk spontaneously on the opposite side of ischemia area, showing no abnormal posture during rest; 3 points, the body tilted or fell to the opposite side of the ischemia area during rest; 4 points, no spontaneous movement; 5 points, death before assessment.

2,3,5-Triphenyltetrazolium Chloride Staining

The procedure for 2,3,5-triphenyltetrazolium chloride (TTC) staining referred to Benedek's method.[8] Starting from the optic chiasma, a slice with a thickness of 2 mm was cut anteriorly, and 4 slices were cut posteriorly. A total of 5 slices were placed into 1% TTC solution, incubated at 37 ℃ in darkness for 30 min, and then transferred into 10% formaldehyde for fixation for 3 h. Image J software (1.53n, National Institutes of Health, USA) was used to calculate the infarct size. According to the formula V = S × D (S is the infarct area of the brain slice, and D is the thickness of the brain slice), the sum of the infarct volume (V) of all the brain slices was taken as the total infarct volume.

Hematoxylin-Eosin Staining

Samples were fixed with 4% paraformaldehyde. After fixation, the samples were pruned, dehydrated, embedded, sliced, stained, and sealed for final microscopic examination. The slices were viewed under a microscope (Eclipse Ci-L, Nikon, Japan) and were observed in detail under 400× magnification.

Construction of AAV and Virus Packaging

Corresponding vectors were selected and target fragment PCR primers were designed. Restriction endonuclease was used for digestion of the vector, and purified linear vectors were recovered using agarose gel electrophoresis. Target fragments were amplified using PCR according to the designed primers, and fragments of the correct size were recovered using agarose gel electrophoresis. The linearized vector and the target fragment were connected using homologous recombination or T4 connection. The DH5a or stbl3 components were transformed by spreading bacteria on a culture plate and culturing for 12–16 h. Single colonies were selected for verification, and the positive clones were verified by sequencing. Selected samples with the correct sequence were used for plasmid extraction; a 3-plasmid AAV system was used for virus packaging. This included the following plasmids: a vector plasmid carrying the target gene or short hairpin RNA; a pAAV-RC vector plasmid; and a pHelper vector plasmid. After high-purity endotoxin-free extraction, the 3 plasmids were co-transfected into 293T cells using Lipofiter™ transfection reagent. Cell precipitations were collected 72 h after transfection and the titer of AAV preservation solution was collected using column purification. Finally, the AAV indicators were determined according to strict quality standards.

Stereotactic Brain Injection

Mice were anesthetized with penotobarbital sodium (50 mg/kg, intraperitoneal injection) and their heads were depilated for skin preparation. The head was fixed firmly in a brain stereotaxic instrument so that the skull was located at the same level for each mouse. Surgical field skin was routinely disinfected with alcohol. The skin was incised to expose the anterior fontanel to the position between the two ears, and

bleeding was carefully stopped and the periosteum was peeled back. The injection site of right lateral ventricle was marked: 0.5 mm behind the fontanelle, 1 mm to the right of the midline of the skull, and 2.5 mm under the dura. The skull was gently drilled into until the dura, and 2-μL AAV preservation solution was injected using a microsyringe. The microsyringe was fixed vertically on the brain stereotaxic instrument, and the needle was inserted slowly and uniformly. When the needle reached the predetermined position, the AAV preservation solution was injected at a constant speed for 15 min. After injection, the needle was remained for 5 min and then slowly removed. The incision was sterilized and sutured after operation. The mice in the MCAO group were injected with miR-7 knockdown AAV or carrier control AAV 3 weeks before operation; the mice in EA group were injected with miR-7 overexpression AAV or an overexpression control AAV.

Immunohistochemistry

Conventional 4-μm brain slices were analyzed according to the instructions of an immunohistochemical kit. Referring to the standards of Weidner,[9] any endothelial cells or endothelial cell clusters labeled with CD34 antibody was counted as one vessel. Each slice was counted in 3 fields. The number of microvessels (microvessel density) was calculated under 400× magnification, and mean values were calculated.

Real-Time PCR

Total RNA was extracted from the cerebral cortex using the TRIzol reagent, and cDNA was synthesized using a reverse transcription reagent. The cDNA was used as template for real-time PCR reaction. Real-time PCR was performed under the following conditions: 95 ℃ 5 min; 40 PCR cycles (95 ℃ 10 s, 60 ℃ 30 s); followed by 95 ℃ for 15 s, 60 ℃ for 1 min, and 95 ℃ for 30 s. U6 was used as the internal reference gene for miR-7, and GAPDH was used as the internal reference gene for VEGF, KLF4, and ANG-2. The relative expression levels of the target genes were calculated using the $2^{-\triangle\triangle CT}$ method. The reverse primers for miR-7 and the primers for U6 were provided in microRNA reverse transcription kit. The primer sequence are shown in Table 1.

Western Blot

For Western blot, 50 mg of cerebral cortex was taken and the lysate was added (RIPA 500 μL + PMSF 5 μL, phosphoprotease inhibitor). Tissue was dissociated and centrifuged for 15 min at 12,000 r/min, and the supernatant was collected. According to the total protein concentration determined using the bicinchoninic acid (BCA) method, the samples were diluted to make the total protein concentration in each group equal. Samples were boiled for 10 min for protein denaturation then cryopreserved at –20 ℃. Protein from boiled samples was separated using 10% SDS-PAGE and transferred to polyvinylidene fluoride (PVDF) membranes. PVDF membranes were incubated in diluted primary antibodies (anti-VEGFA: 1:1,000, anti-KLF4: 1:1,000, anti-ANG2: 1:1,000) for 16 h, and then incubated in secondary antibodies (mouse anti-rabbit: 1:10,000) with nutation at room temperature for 1 h. After 3 washes in 1× tris-buffered saline with Tween-20 (TBST) for 10 min each, membranes were immersed in development solution for several seconds and analyzed using the Bio-Rad gel imaging system (Tanon 1200, Tanon, China).

Table 1. Primer Sequence of Real-Time PCR

Gene	Primers	Length
miR-7	F: 5'-CGCAGTGGAAGACTAGTGA-3'	19 bp
VEGF	F: 5'-GACTATTCAGCGGACTCACCA-3'	21 bp
	R: 5'-TGAGGGAGTGAAGAACCAACC-3'	21 bp
KLF4	F: 5'-GTGCCCCGACTAACCGTTG-3'	19 bp
	R: 5'-GTCGTTGAACTCCTCGGTCT-3'	20 bp
ANG-2	F: 5'-AAGGAAGCCCTTATGGACGAA-3'	21 bp
	R: 5'-GGGGAGACCTTCCTTTGTGT-3'	20 bp
GAPDH	F: 5'-AGGTCGGTGTGAACGGATTTG-3'	21 bp
	R: 5'-TGTAGACCATGTAGTTGAGGTCA-3'	23 bp

Notes: F: forward; R: reverse

Statistical Analysis

Data are presented as mean ± standard deviation ($\bar{x} \pm s$). Data normality was assessed using Shapiro–Wilk test. The homogeneity of variances was analyzed using the Levene test. For multiple comparisons, one-way analysis of variance and least significant difference (LSD) test were applied. Statistical significance was considered for *P*-values less than 0.05. GraphPad Prism (v.8.0.2; GraphPad Inc., USA) and SPSS (v24; IBM Corp., USA) were used for statistical analysis.

RESULTS

Therapeutic Effects of EA in Mouse Model of Cerebral Ischemia

The mean neurological deficit score of the sham group was 0 at 2 h and 3 d after the operation. The mice in the MCAO and EA groups showed varying

degrees of neurological deficits 2 h after operation. The neurological deficit scores of the MCAO and EA groups were significantly higher than the sham group at 2 h and 3 d after the operation. At 3 d after operation, the neurological deficit scores of the EA group were significantly lower than that at 2 h after operation, and significantly lower than those of the MCAO group (P<0.01, Figure 1A). At 3 d after operation, cerebral infarction volumes in the MCAO group were significantly higher than those in the sham group; while the EA group were significantly lower than the MCAO group (P<0.01, Figures 1B and 1C).

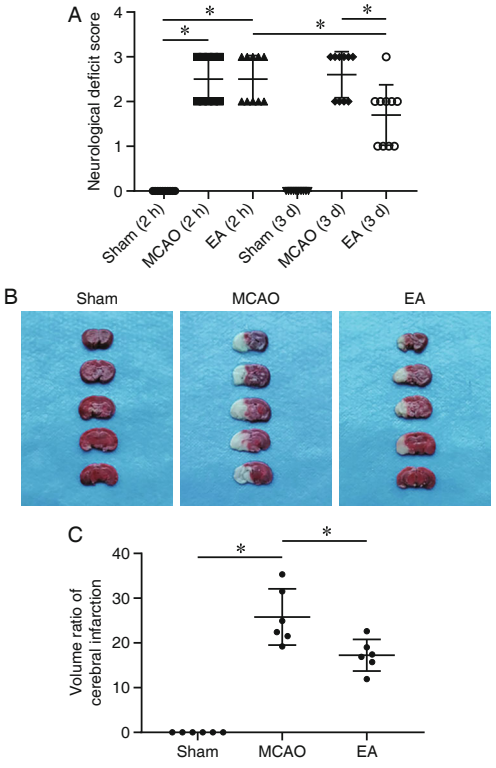

Figure 1. Neurological Function and Infarction Area Analysis after MCAO

Notes: A: neurological deficit scores in mice ($\bar{x} \pm s$, n=10); B: TTC staining results; C: cerebral infarct volume in mice 3 d after MCAO induction ($\bar{x} \pm s$, n=6). MCAO: middle cerebral artery occlusion; EA: electroacupuncture; the same below; *P<0.01

The following basic pathological changes were seen in the tissue slices 3 d after the operation. In the sham group, there was no obvious infarct; the brain membranes were intact, and the number of neurons was high, with no obvious hemorrhaging or other abnormalities. In the MCAO group, the right cerebral cortex showed a wide range of infarction and tissue edema. The tissue was stained lightly by HE staining. In the infarct area, the nerve fibers were loose, and the number of neurons was greatly reduced, with massive neuronal necrosis including nucleus shrinkage, fragmentation, and missing nuclei. The cytoplasm was eosinophilic. In the EA group, some nucleus shrinkage could be seen in the cerebral cortex, with light HE staining of the tissue. In the infarct area, the nerve fibers were loose and the number of neurons was decreased with neuronal necrosis, nucleus shrinkage, fragmentation, and missing nuclei. The cytoplasm was eosinophilic (Figure 2A). At the same time point, the cerebral microvascular density in the MCAO group was significantly increased compared to the sham group, and that in the EA group was even higher (P<0.01, Figures 2B and 2C).

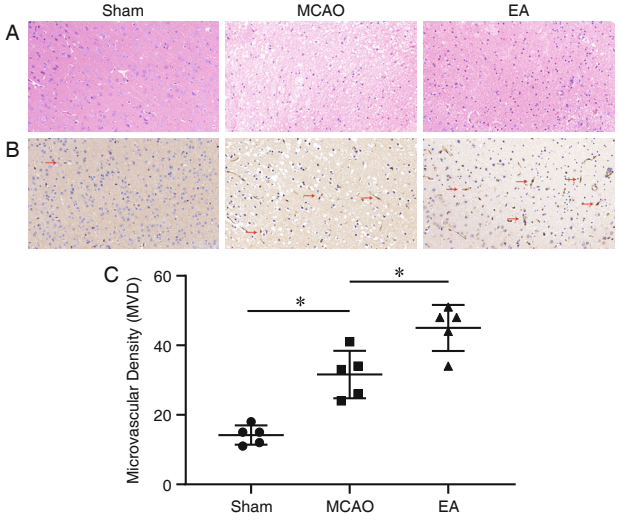

Figure 2. Histopathological Changes of Mice and Microvessel Density Analysis in Each Group

Notes: A: hematoxylin-eosin staining under 400× magnification; B: immunohistochemistry under 400× magnification; C: microvessel density in mouse brains 3 d after MCAO induction ($\bar{x} \pm s$, n=5); *P<0.01

EA Promoted Angiogenesis

According to the PCR results, the expression of miR-7 in the MCAO group (3 d after the operation) was significantly increased compared to the sham group, while that in the EA group was significantly decreased compared to the MCAO group (Figure 3A). PCR and Western blot showed that the expression levels of KLF4/VEGF and ANG-2 (downstream target gene of miR-7) in the MCAO group were significantly decreased at 3 d after operation, while the expression levels of the corresponding indexes in the EA group were significantly increased (P<0.05 or 0.01, Figures 3B–3D, Figure 4).

miR-7 AAV Verification

PCR verification showed that the expression of miR-7 in the cortex was upregulated after the injection of an miR-7 overexpression AAV and was downregulated after the injection of an miR-7 knock down AAV (Figure 5).

Chin J Integr Med 2024 Jun;30(6):543-550

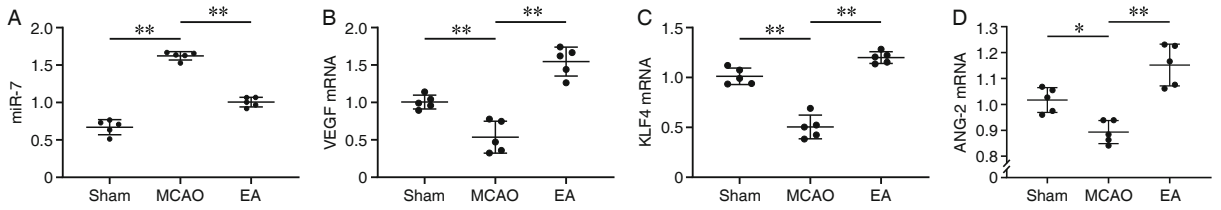

Figure 3. Expression of miR-7 (A), VEGF (B), KLF4 (C) and ANG-2 mRNAs (D) 3 d after Model Induction in Mice by Real Time PCR ($\bar{x} \pm s$, n=5)

Notes: miR-7: miRNA-7; VEGF: vascular endothelial growth factor; KLF4: Krüppel-like factor 4; ANG-2: angiopoietin-2; the same below. $^{*}P$<0.05, $^{**}P$<0.01

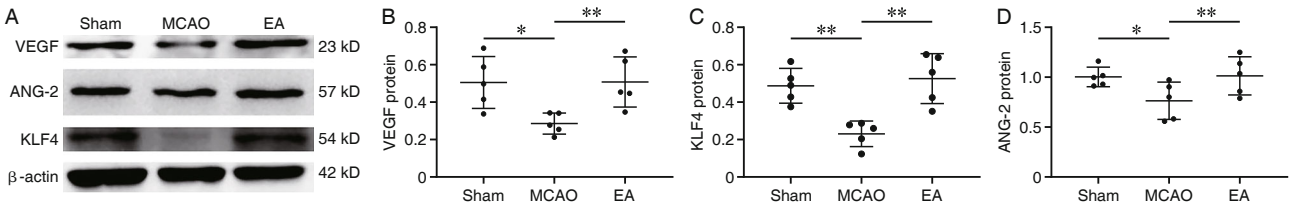

Figure 4. Protein Expression of miR-7 Downstream Target Genes in Mice 3 d after Model Induction by Western Blot ($\bar{x} \pm s$, n=5)

Notes: Electrophoretic band diagram of proteins (A); protein expressions of VEGF (B), KLF4 (C), ANG-2 (D). $^{*}P$<0.05, $^{**}P$<0.01

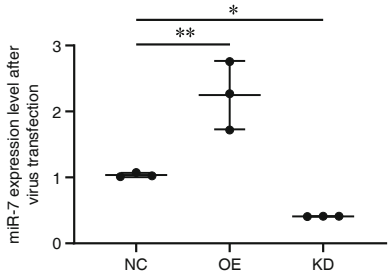

Figure 5. Expression of miR-7 in Mice Cerebral Cortex after Transfection with miR-7 Overexpression or Knockdown AAVs ($\bar{x} \pm s$, n=3)

Notes: AAVs: adeno-associated viruses; NC: carrier control group; KD: miR-7 knockdown group; OE: miR-7 overexpression groups $^{*}P$<0.05, $^{**}P$<0.01

EA Inhibited miR-7 to Promote Angiogenesis

After transfection of the miR-7 overexpression and knock down AAVs, the mRNA expression levels of KLF4, VEGF, and ANG-2 in the MCAO+KD group at 3 d were significantly higher than those in MCAO+NC group. The mRNA expressions of KLF4, VEGF, and ANG-2 in the EA+OE group at 3 d were significantly lower than those in the EA+NC group (Figures 6 and 7).

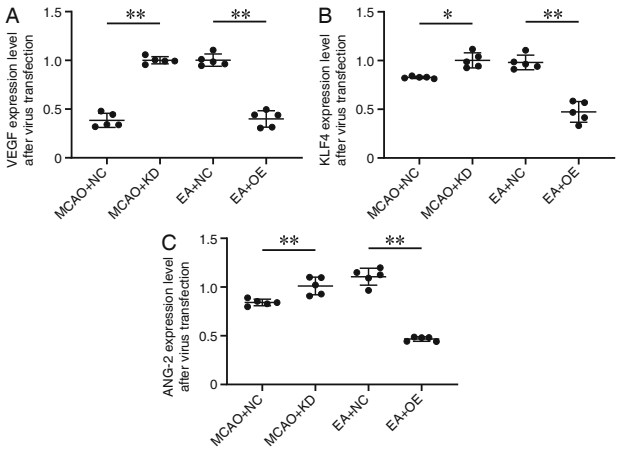

Figure 6. mRNA Expression of miR-7 Downstream Target Genes VEGF (A), KLF4 (B) and ANG-2 (C) in Mice after Transfection with miR-7 Overexpression or Knockdown AAVs ($\bar{x} \pm s$, n=5)

Notes: MCAO+NC: model and carrier control group; MCAO+KD: model and miR-7 knockout group; EA+NC: electroacupuncture treatment and carrier control group; EA+OE: electroacupuncture treatment and miR-7 overexpression group; $^{*}P$<0.05, $^{**}P$<0.01

DISCUSSION

Ischemic brain injury belongs to the category

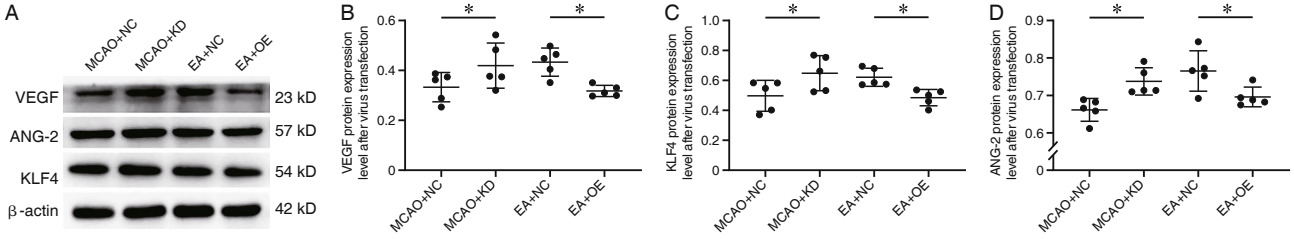

Figure 7. Protein Expression of miR-7 Downstream Target Genes after Transfection with miR-7 Overexpression or Knockdown AAVs by Western Blot ($\bar{x} \pm s$, n=5)

Notes: Electrophoretic bands showing protein expression (A); expression of VEGF protein (B), KLF4 protein (C), and ANG-2 protein (D); $^{*}P$<0.05

of "stroke" in Chinese medicine (CM). Based on the theory of acupuncture and moxibustion, it needs to be treated from the brain, and the Governor vessel points are considered to be the main points in the selection of acupoints. GV 26, the meeting point of the Governor vessel and the Yangming meridian, is an important clinical first-aid point, as it may increase cerebral blood flow and regulate vascular activity.[10] Acupuncture at GV 26 is one of the most commonly used therapeutic strategies as a single point treatment for stroke.

Angiogenesis refers to the process of generating new blood vessels, and it forms a mature capillary network through the proliferation and migration of endothelial cells. It is an important process in nerve repair after cerebral ischemia and participates in the recovery of nerve function. Therefore, angiogenesis interventions in the early stages of cerebral ischemia can significantly improve patient prognosis. EA is a combination of CM and modern technology and has been widely used in the treatment of various diseases including ischemic stroke.[11] Evidence has demonstrated that EA can promote angiogenesis and improve functional outcomes after cerebral ischemia.[12] EA was shown to upregulate VEGF expression through acetylation of H3K9 on the VEGF promoter,[13] activate angiogenesis,[14-16] alleviate learning and memory impairments,[17] and prolong the thrombolysis time window.[18,19] Thus, the mechanisms of EA may be related to increasing VEGF expression and promoting the establishment of collateral circulation.[20,21] This study mainly explored the effects of EA at GV 26 on angiogenesis in a mouse model of MCAO. The results showed that EA at GV 26 could improve neurological deficit scores of cerebral ischemia mice, inhibit the increase of cerebral infarction volumes, and increase cerebral microvascular density, thereby improving cerebral ischemia injury. Its mechanism may be related to the inhibition of miR-7 expression.

The miR-7 gene is located in the intron region of human Heterogeneous nuclear ribonucleoprotein K (HNRNPK) on human chromosome 9, which is highly conserved. miR-7 can regulate the biological function of many cells, especially in the process of endothelial cell angiogenesis. The target genes of miR-7, which are closely related to angiogenesis and have high differential expression multiples in the acupuncture treatment group, are KLF4 and ANG-2, and KLF4 can regulate VEGF. Modern studies have shown that miR-7 can inhibit angiogenesis.[22,23] Silencing miR-7 could upregulate VEGF to promote angiogenesis,[1] while overexpression of miR-7 had the opposite effect.[24] The expression levels of members of the KLF4/VEGF pathway increased after downregulation of miR-7, suggesting that KLF4 can regulate VEGF and participate in angiogenesis.[1] ANG-2 activates Tie-2 and induces its phosphorylation, which promotes multiple myeloma-associated angiogenesis in bone marrow.[2]

In order to further demonstrate that EA at GV 26 promotes angiogenesis by inhibiting the expression of miR-7, this study used brain stereotactic injection of AAVs to further verify the role of miR-7 in cerebral ischemia. By injecting an miR-7 knockdown AAV in the MCAO group, it was found that downregulation of miR-7 could improve cerebral ischemic injury, which had the same therapeutic effects as EA at GV 26. The overexpression of miR-7 in the EA group reversed the therapeutic effects of EA. Therefore, EA at GV 26 may relieve the inhibition of miR-7 on the downstream target genes KLF4/VEGF and ANG-2 by downregulating the expression level of miR-7 and promote angiogenesis. Therefore, acupuncture at GV 26 can promote angiogenesis by downregulating the expression of miR-7 and relieve its inhibitory effects on the downstream target genes KLF4/VEGF and ANG-2.

The present study found that EA at GV 26 can inhibit the expression of miR-7 that is induced by cerebral ischemia, promote the expression of KLF4/VEGF and ANG-2, and in turn promote angiogenesis. This study provided sufficient evidence for the mechanisms of EA in the treatment of cerebral ischemia. However, it had some limitations. Cerebral ischemia in mice can cause abnormal expression of a series of miRNAs and target genes that are involved in the regulation of ischemic brain injury. This study only analyzed changes in expression of miR-7, KLF4/VEGF, and ANG-2 and their role in the promotion of angiogenesis after EA at GV 26. In addition, due to the limitations of the treatment, this study did not explore whether miR-7 affects angiogenesis by regulating KLF4/VEGF and ANG-2 *in vitro*.

In conclusion, we found that miR-7 displayed altered expression in a mouse model of MCAO, suggesting that it may be implicated in the development of cerebral ischemic injury. We further found that inhibiting the expression of miR-7 could promote the expression of the downstream target genes KLF4/

VEGF and ANG-2, and these factors were related to the promotion of cerebral angiogenesis. A better understanding of the mechanisms of miR-7 can provide a new therapeutic target for cerebral ischemic diseases.

Conflict of Interest

The authors confirm that there is no conflict of interest related to the manuscript.

Author Contributions

Zhou S and Shu S independently designed the study. Yu Q and Ju XY carried out the experiment. Yu Q, Peng W, Ren XQ, Si SH, Song SZ, Xie XY collected and analyzed the data. Yu Q wrote the initial draft of the paper. Shu S and Fang BJ assisted with refinement of the manuscript. All authors approved the final version of the paper.

Availability of Data and Material

The data that support the findings of this study are available from the corresponding author upon reasonable request.

REFERENCES

1. Li YZ, Wen L, Wei X, Wang QR, Xu LW, Zhang HM, et al. Inhibition of miR-7 promotes angiogenesis in human umbilical vein endothelial cells by upregulating VEGF via KLF4. Oncol Rep 2016;36:1569-1575.
2. Belloni D, Marcatti M, Ponzoni M, Ciceri F, Veschini L, Corti A, et al. Angiopoietin-2 in bone marrow milieu promotes multiple myeloma-associated angiogenesis. Exp Cell Res 2015;330:1-12.
3. Zhu W, Ye Y, Liu Y, Wang XR, Shi GX, Zhang S, et al. mechanisms of acupuncture therapy for cerebral ischemia: an evidence-based review of clinical and animal studies on cerebral ischemia. J Neuroimmune Pharmacol 2017;12:575-592.
4. Russell WMS, Burch RL, eds. The principles of humane experimental technique. London: Methuen; 1959.
5. Hata R, Mies G, Wiessner C, Fritze K, Hesselbarth D, Brinker G, et al. A reproducible model of middle cerebral artery occlusion in mice: hemodynamic, biochemical, and magnetic resonance imaging. J Cereb Blood Flow Metab 1998;18:367-375.
6. Li CR, Hua XB, Song DL, Zhou HL, Hu YL. Commonly used acupuncture points in mice. Exp Anim Anim Exp (Chin) 1992;2:85-87.
7. Hunter AJ, Hatcher J, Virley D, Nelson P, Irving E, Hadingham SJ, et al. Functional assessments in mice and rats after focal stroke. Neuropharmacology 2000;39:806-816.
8. Benedek A, Móricz K, Jurányi Z, Gigler G, Lévay G, Hársing LG Jr, et al. Use of TTC staining for the evaluation of tissue injury in the early phases of reperfusion after focal cerebral ischemia in rats. Brain Res 2006;1116:159-165.
9. Weidner N, Semple JP, Welch WR, Folkman J. Tumor angiogenesis and metastasis—correlation in invasive breast carcinoma. N Engl J Med 1991;324:1-8.
10. Li J, Zhang M, He Y, Du YH, Zhang XZ, Georgi R, et al. Molecular mechanism of electroacupuncture regulating cerebral arterial contractile protein in rats with cerebral infarction based on MLCK pathway. Chin J Integr Med 2023;29:61-68.
11. Chen B, Lin WQ, Li ZF, Zhong XY, Wang J, You XF, et al. Electroacupuncture attenuates ischemic brain injury and cellular apoptosis via mitochondrial translocation of cofilin. Chin J Integr Med 2021;27:705-712.
12. Li J, Chen L, Li D, Lu M, Huang X, Han X, et al. Electroacupuncture promotes the survival of the grafted human MGE neural progenitors in rats with cerebral ischemia by promoting angiogenesis and inhibiting inflammation. Neural Plast 2021;2021:4894881.
13. Fu SP, He SY, Xu B, Hu CJ, Lu SF, Shen WX, et al. Acupuncture promotes angiogenesis after myocardial ischemia through H3K9 acetylation regulation at VEGF gene. PLoS One 2014;9:e94604.
14. Feng R, Zhang F. The neuroprotective effect of electro-acupuncture against ischemic stroke in animal model: a review. Afr J Tradit Complement Altern Med 2014;11:25-29.
15. Abali AE, Cabioglu T, Bayraktar N, Ozdemir BH, Moray G, Haberal M. Efficacy of acupuncture on pain mechanisms, inflammatory responses, and wound healing in the acute phase of major burns: an experimental study on rats. J Burn Care Res 2022;43:389-398.
16. Hong H, Yue JM, Zhang WJ, Zhu BM. Epigenetic mechanisms of angiogenesis in the ischemic heart diseases with acupuncture treatment. Med Acupunct 2020;32:381-384.
17. Wu Y, Hu R, Zhong X, Zhang A, Pang B, Sun X, et al. Electric acupuncture treatment promotes angiogenesis in rats with middle cerebral artery occlusion through ephb4/ephrinb2 mediated Src/PI3K signal pathway. J Stroke Cerebrovasc Dis 2021;30:105165.
18. Chang SQ, Zhang XC, Zhang A, Song YY, Jiang SY, Zhang ZH, et al. Acupuncture intervention prolongates thrombolysis time window by regulating cerebral cortex angiogenesis-related genes and proteins in cerebral infarction rats. Acupunct Res (Chin) 2021;46:751-756.
19. Gu YH, Zhang XC, Xu WT, Zhang A, Zhang ZH, Jiang SY, et al. Effect of acupuncture on neurological function, cerebral infarction volume, thrombolysis time window and cerebral cell apoptosis signaling pathway in cerebral infarction rats. Acupunct Res (Chin) 2020;45:209-214.
20. Tang YL, Liu ML, Luo J, Li N, Zhang GS,Yu J, et al. Exploring the effect of acupuncture plus mild hypothermia on miRNA-204 and its target gene expressions in CIRI rat brain tissues based on MAPK signal pathway. J Acupunct Tuina Sci 2021;19:338-344.
21. Shi L, Cao HM, Li Y, Xu SX, Zhang Y, Zhang Y, et al. Electroacupuncture improves neurovascular unit reconstruction by promoting collateral circulation and angiogenesis. Neural Regen Res 2017;12:2000-2006.
22. Lin J, Liu Z, Liao S, Li E, Wu X, Zeng W. Elevated microRNA-7 inhibits proliferation and tumor angiogenesis and promotes apoptosis of gastric cancer cells via repression of Raf-1. Cell Cycle 2020;19:2496-2508.
23. Babae N, Bourajjaj M, Liu Y, Van Beijnum JR, Cerisoli F, Scaria PV, et al. Systemic miRNA-7 delivery inhibits tumor angiogenesis and growth in murine xenograft glioblastoma. Oncotarget 2014;5:6687-6700.
24. Fan X, Liu M, Tang H, Leng D, Hu S, Lu R, et al. MicroRNA-7 exerts antiangiogenic effect on colorectal cancer via ERK signaling. J Surg Res 2019;240:48-59.

(Accepted May 31, 2023; First Online March 27, 2024)
Edited by YUAN Lin